Luminescent Complexes Hot Paper

International Edition: DOI: 10.1002/anie.201504894
German Edition: DOI: 10.1002/ange.201504894

$[Cr(ddpd)_2]^{3+}$: A Molecular, Water-Soluble, Highly NIR-Emissive Ruby Analogue

Sven Otto, Markus Grabolle, Christoph Förster, Christoph Kreitner, Ute Resch-Genger, and Katja Heinze**

Abstract: *Bright, long-lived emission from first-row transition-metal complexes is very challenging to achieve. Herein, we present a new strategy relying on the rational tuning of energy levels. With the aid of the large N-Cr-N bite angle of the tridentate ligand ddpd (N,N′-dimethyl-N,N′-dipyridine-2-ylpyridine-2,6-diamine) and its strong σ-donating capabilities, a very large ligand-field splitting could be introduced in the chromium(III) complex $[Cr(ddpd)_2]^{3+}$, that shifts the deactivating and photoreactive $^4T_2$ state well above the emitting ^2E state. Prevention of back-intersystem crossing from the ^2E to the $^4T_2$ state enables exceptionally high near-infrared phosphorescence quantum yields and lifetimes for this 3d metal complex. The complex $[Cr(ddpd)_2](BF_4)_3$ is highly water-soluble and very stable towards thermal and photo-induced substitution reactions and can be used for fluorescence intensity- and lifetime-based oxygen sensing in the NIR.*

Dyes with room-temperature emission in the near infrared (NIR) spectral region (> 650 nm) have emerged as promising candidates for NIR organic light emitting diodes (OLEDs), fiber-optic telecommunication applications, night-vision readable displays, security inks for identification systems, oxygen sensing, and in vivo imaging.[1–7] Essentially, all currently employed (water-)soluble, NIR emissive dyes are based on lanthanide complexes,[4–7] complexes of the second- and third-row metal ions,[8–10] complex organic scaffolds,[11] or a combination of them.[12] All of them feature specific advantages, such as long-lived emissive states and large energy differences between absorption and emission maxima (lanthanides, 4d/5d metal complexes), medium to high quantum yields, and rational tuning of the emission energy (organic dyes). Typical drawbacks are, however, multi-step syntheses and poor water solubility and dye aggregation for the more extended π-systems required for NIR emission (organic dyes),[11h] short lifetimes in the range of 1–10 ns (organic dyes, many transition-metal complexes), or high costs (e.g. Eu, Rh, Ir, Ru, Os, Pd, Pt, Au). Furthermore, NIR emitters typically suffer from radiationless relaxation to the ground state (energy gap law).[13] An emerging class of luminophores comprises first-row transition-metal complexes. They are, however, limited to complexes of d^{10} ions (Zn^{II}, Cu^{I}), such as [Zn(tpp)] or $[Cu(PPh_3)_2(phen)]^+$ (tpp = *meso*-tetraphenylporphyrinato, phen = 1,10-phenanthroline) derivatives with quantum yields around 2–3 %, lifetimes in the nanosecond range,[1] and in most cases emission in the visible. Although considerable progress has been made in the field of Cu^{I} complexes.[14] Octahedral Cr^{III} complexes[15] have been also suggested as NIR emitters partly because the Cr^{III} emission in solid materials, such as chromium-doped sapphire (ruby), has led to the historically important development of the ruby laser in 1960.[16] The phosphorescence quantum efficiencies for most of these complexes were, however, too low ($\Phi < 0.1\,\%$) for practical applications[1] despite the fascinating photophysical aspects observed in $[Cr(ox)_3]^{3-}$ (ox = oxalato) polymeric networks[17a,b] and the use of Cr^{III} complexes as energy donors for lanthanide emission in heterometallic complexes.[17c–e] $[Cr(bpy)_3]^{3+}$ and $[Cr(phen)_3]^{3+}$ (byp = 2,2′-bipyridine) complexes have recently found renewed interest as photoredox catalysts.[18]

The reasons for the poor quantum yields of Cr^{III} complexes can be understood from ligand field theory.[15] The desired luminescence of octahedral d^3 Cr^{III} complexes with a $(t_{2g})^3(e_g)^0$ electron configuration occurs from a transition from doublet states (^2E and $^2T_1$) to the quartet ground state ($^4A_2$), in the red to near-infrared spectral region (for simplicity, we use the O_h point-group classification). The ^2E and $^2T_1$ spectroscopic terms as well as the $^4A_2$ ground term arise from the $(t_{2g})^3$ electron configuration and hence, the geometric reorganization is very minor, yielding sharp emission bands like the ruby emission.[16] At low ligand-field strength, the doublet states lie above the $^4T_2$ state of electron configuration $(t_{2g})^2(e_g)^1$ yielding weak, broad fluorescence from $^4T_2$ instead.[19] Even for classical strong-field ligands, such as bpy, phen, or 2,2′:6′,2″-terpyridine (tpy), the energy difference between $^4T_2$ and the emitting $^2E/^2T_1$ states is so small that back-intersystem crossing occurs, strongly reducing phosphorescence quantum yields and lifetimes.[1,15] Furthermore, the $^4T_2$ state is prone to photosubstitution and hence, its back-population should be avoided.[15,20] To increase the phosphorescence quantum yield, the energy difference between the $^4T_2$ and ^2E states should be large to prevent back-intersystem crossing to the detrimental $^4T_2$ state. This should be achievable by a using a strong ligand-field to shift

---

[*] S. Otto, Dr. C. Förster, C. Kreitner, Prof. K. Heinze
Institute of Inorganic and Analytical Chemistry
Johannes Gutenberg-University of Mainz
Duesbergweg 10–14, 55128 Mainz (Germany)
E-mail: katja.heinze@uni-mainz.de

Dr. M. Grabolle, Dr. U. Resch-Genger
Division 1.10
Federal Institute for Materials Research and Testing (BAM)
Richard-Willstätter-Strasse 11, 12489 Berlin (Germany)
E-mail: ute.resch@bam.de

C. Kreitner
Graduate School Materials Science in Mainz
Staudingerweg 9, 55128 Mainz (Germany)

Supporting information for this article is available on the WWW under http://dx.doi.org/10.1002/anie.201504894.

the $^4T_2$ state to higher energy in conjunction with a strong nephelauxetic effect lowering the energy of the doublet states ^2E and $^2T_1$ and hence should be made possible by proper ligand design.

Recently, we introduced the tridentate ddpd ligand (*N,N′*-dimethyl-*N,N′*-dipyridin-2-ylpyridine-2,6-diamine) with a large bite angle N-M-N of around 90° in six-coordinate metal complexes to optimize metal–ligand orbital overlap and to induce a stronger ligand field compared to bpy or tpy (Scheme 1).[21] Also, ddpd is a poor π-acceptor ligand, that is, rather electron rich and difficult to reduce, but a quite strong σ-donor ligand.[21] With these properties of ddpd in mind, we envisaged that ddpd could increase the energy of the $^4T_2$ state in a $[Cr(ddpd)_2]^{3+}$ complex $\mathbf{1}^{3+}$ (Scheme 1) and simultaneously decrease the energy of the ^2E state, resulting in an enlarged $^4T_2/^2E$ energy gap, which impedes back-intersystem crossing.

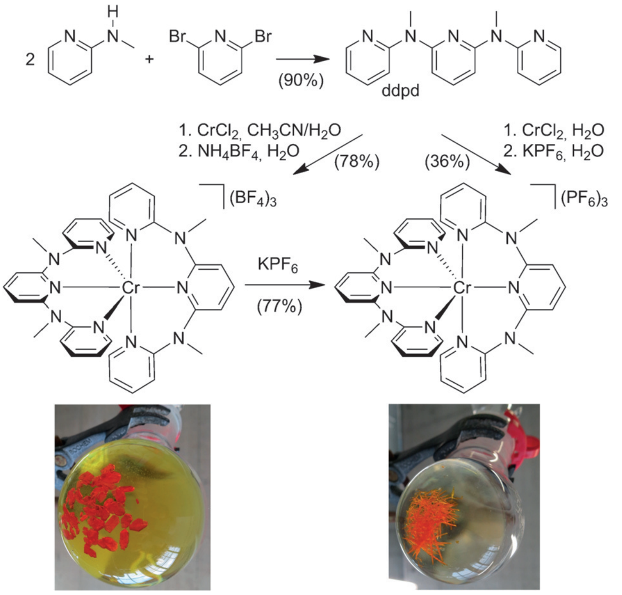

Scheme 1. High-yield syntheses of $\mathbf{1}(X)_3$ and photographs of crystals of $\mathbf{1}(X)_3$ grown from CH_3CN solutions.

$[Cr(bpy)_3]^{3+}$ and $[Cr(tpy)_2]^{3+}$ are substitutionally labile under alkaline conditions giving the hydroxido complexes $[Cr(bpy)_2(OH)_2]^+$ and $[Cr(tpy)(OH)_x]_n^{(3-x)n}$.[22] Possibly, the π-accepting ligands bpy and tpy reduce the electron density between the ligand axes by back-donation from t_{2g} orbitals, facilitating a nucleophilic attack of hydroxide. The π-accepting nature of bpy/tpy also accounts for the special redox properties, as reduction of $[Cr^{III}(bpy)_3]^{3+}$ or $[Cr^{III}(tpy)_2]^{3+}$ does not yield Cr^{II}, Cr^{I}, Cr^{0}, Cr^{-I} oxidation states but is ligand centered.[23] The envisaged ddpd complex $\mathbf{1}^{3+}$ should resist ligand-centered reductions and nucleophilic attack at the metal center due to the strong electron donating power of ddpd.

The synthesis of $\mathbf{1}^{3+}$ is straightforward from $CrCl_2$ and ddpd[21a] in water. Ion exchange with $(BF_4)^-$ or $(PF_6)^-$ gives the bright orange salts $\mathbf{1}(BF_4)_3$ and $\mathbf{1}(PF_6)_3$ (Scheme 1, Supporting Information). Both were obtained as single crystals suitable for X-ray diffraction analysis (Figure 1, Supporting Information, Figure S1). The complex cations feature an essentially octahedral CrN_6 coordination geometry with Cr–N distances of 2.028–2.054 Å and N-Cr-N angles close to 90° and 180° as required for a large ligand-field splitting. Similar to structurally comparable $[M(ddpd)_2]^{2+}$ complexes, the ligands are wrapped around the metal center (Figure 1) and the counter ions fill the pockets between the ligands with Cr···B/P distances between 5.3 and 7.0 Å (Supporting Information, Figure S1).[21]

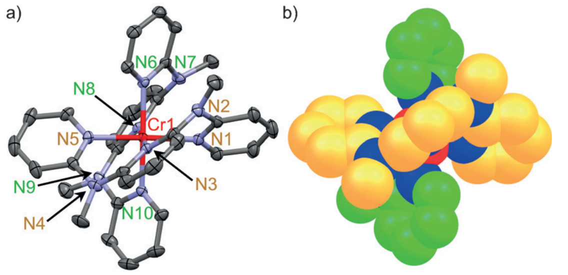

Figure 1. a) Molecular structure of the cation of $\mathbf{1}(BF_4)_3$ in the solid state (thermal ellipsoids set at 50% probability); b) space-filling representation of $\mathbf{1}^{3+}$ with the two ligands are shown in yellow and green, respectively (hydrogen atom omitted for clarity).

Magnetic susceptibility and EPR data are consistent with a quartet ground state ($\chi T = 1.833\ cm^3\,K\,mol^{-1}$ at 300 K; $g_{av} = 1.990$ at 77 K, Figure S14, Supporting Information) similar to $[Cr(tpy)_3]^{3+}$.[24] A reversible $Cr^{III/II}$ reduction is observed at −1.11 V versus ferrocene (Supporting Information, Figure S13). Compared to $[Cr(bpy)_3]^{3+}$ ($E_{1/2} = -0.63$ V) and $[Cr(tpy)_2]^{3+}$ ($E_{1/2} = -0.53$ V), this reduction occurs at much more negative potential.[23] DFT calculations (B3LYP, RIJ-COSX, Def2-SVP/J, Def2-SVP, ZORA) confirm the metal-centered reduction to Cr^{II} (Supporting Information, Figure S25,S26). The next reduction at $E_p = -1.94$ V is irreversible as coordinated ddpd cannot be reduced to its radical anion. Interestingly, $\mathbf{1}(BF_4)_3$ is highly soluble in water (0.0479 mol L^{-1}) while $\mathbf{1}(PF_6)_3$ is more soluble in CH_3CN (0.208 mol L^{-1}), enabling different applications of the two salts. The absorption spectra of $\mathbf{1}^{3+}$ in H_2O or CH_3CN show maxima at 220(sh), 302, 315(sh), 350(sh), and 435 nm (Figure 2, Supporting Information, Figure S5) which can be assigned to ππ*, ligand-to-metal charge transfer (LMCT) and mixed metal-centered (MC)/LMCT excitations according to time-dependent DFT calculations (Supporting Information, Figure S20). No metal-to-ligand charge transfer (MLCT) transitions were identified in this energy region because of the weak electron-accepting properties of ddpd and the inaccessible $Cr^{III/IV}$ oxidation. The low-energy absorption maximum is ascribed to the $^4A_2 \rightarrow ^4T_2$ transition (TD-DFT: 427.7, 436.9, and 439.0 nm) and an LMCT (Supporting Information, Figure S20). Three Laporte- and spin-forbidden transitions are found at 697, 736, and 776 nm in the single-crystal absorption spectrum of $\mathbf{1}(BF_4)_3$. These are assigned to $^4A_2 \rightarrow ^2T_2$(tentative), $^2T_1$, and ^2E excitations (Supporting Information, Figure S10). Excitation of a solution of $\mathbf{1}(BF_4)_3$ in water or CH_3CN (Supporting Information, Figure S8) at 435 nm leads to emission spectra that can be superimposed, as

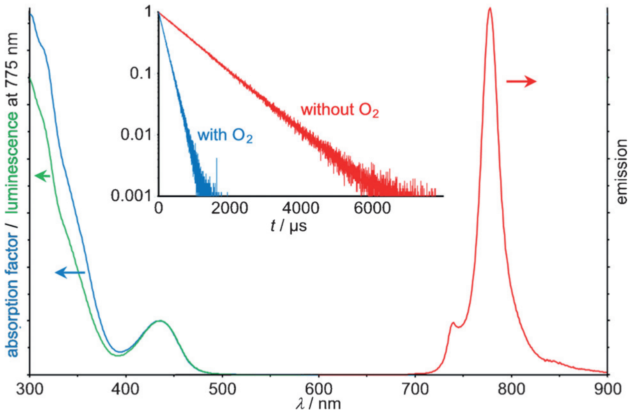

Figure 2. Absorption factor (blue), excitation ($\lambda_{obs} = 775$ nm, green) and emission spectrum ($\lambda_{exc} = 435$ nm, red) of **1**$(BF_4)_3$ in deaerated H_2O at room temperature; the inset shows the emission decay curves of **1**$(BF_4)_3$ in H_2O with and without O_2.

depicted in Figure 2 for CH_3CN. The strong, sharp emission band at 775 nm (full width at half maximum height (FWHM) = 420 cm^{-1}) is ascribed to the ^2E emission and the weaker band at 738 nm to the $^2T_1$ emission.[15,25] A single crystal of **1**$(BF_4)_3$ emits at 740 and 778 nm (Supporting Information, Figure S11). Clearly, these two intraconfigurational doublet states equilibrate at room temperature both in solution and in the solid state. At 100 K in a frozen butyronitrile glass, only the ^2E emission at 779 nm is observed (Supporting Information, Figure S9). The emission of $\mathbf{1}^{3+}$ is considerably red shifted relative to $[Cr(bpy)_3]^{3+}$ (727 nm) and $[Cr(phen)_3]^{3+}$ (730 nm), but similar to that of $[Cr(tpy)_2]^{3+}$ (770 nm).[1,15] The solid material ruby emits at 694 nm.[16]

The luminescence quantum yields (Φ) of $\mathbf{1}^{3+}$ in deaerated CH_3CN and H_2O were determined absolutely with an integrating-sphere setup to $\Phi = 12.1\,\%$ and 11.0 %, respectively. In D_2O, Φ increases to 14.2 %. To our knowledge, these Φ values are by far the highest values reported for Cr^{III} complexes in solution at room temperature to date.[1,15] For instance, $[Cr(bpy)_3]^{3+}$, $[Cr(phen)_3]^{3+}$, and $[Cr(tpy)_2]^{3+}$ have $\Phi = 0.089\,\%$, 0.15 %, and $< 0.00089\,\%$ in water.[1] The lifetimes (τ) of the emitting doublet states of $\mathbf{1}^{3+}$ were determined to $\tau = 899$, 898, and 1164 µs in deaerated CH_3CN, in H_2O, and in D_2O, respectively. Again, these are the highest values reported to date for a molecular Cr^{III} complex in solution at room temperature. The lifetimes of $[Cr(bpy)_3]^{3+}$, $[Cr(phen)_3]^{3+}$, and $[Cr(tpy)_2]^{3+}$ are $\tau = 63$ µs, 270 µs, and $\leqslant 30$ µs, respectively.[1] The solid laser material ruby has $\tau = 4270$ µs[16] while a single crystal of **1**$(BF_4)_3$ reveals $\tau = 443$ µs.

Excitation spectra recorded at 775 nm in CH_3CN and H_2O perfectly match with the absorption spectrum around the 435 nm maximum (Figure 2, Supporting Information, Figure S8) suggesting efficient population of the $^2E/^2T_1$ states from these $^4T_2$ ligand-field and LMCT states. At higher energies, the excitation spectra deviate from the absorption factor suggesting that not all high-energy states of $\mathbf{1}^{3+}$ populate the $^2E/^2T_1$ states. Excitation at 435 nm also yields a very weak broad emission band around 500 nm with τ of 3 ns, independent of the presence of O_2 (Supporting Information, Figure S7). As ddpd emits at 398 nm in CH_3CN ($\Phi = 8.0\,\%$, $\tau = 3.0$ ns; Supporting Information, Figure S12), the weak 500 nm emission cannot be assigned to ddpd fluorescence but is ascribed to the spontaneous $^4T_2 \rightarrow {}^4A_2$ fluorescence of $\mathbf{1}^{3+}$. Delayed $^4T_2 \rightarrow {}^4A_2$ fluorescence[15,19] fed by back-intersystem crossing from $^2E/^2T_1$ states is ruled out on the basis of the short lifetime. Hence, back-intersystem crossing is efficiently prevented in $\mathbf{1}^{3+}$ which accounts for its exceptionally high quantum yield and lifetime. The minimal energy difference between the relaxed ^2E and $^4T_2$ states is estimated at around 7100 cm^{-1} (0.88 eV; 85 kJ mol^{-1}) from the emission spectra. Although the geometry of the ^2E state is close to that of the $^4A_2$ ground state, a large reorganization energy barrier is expected as the relaxed $^4T_2$ state features a Jahn–Teller distorted octahedron with $Cr-N_{ax}$ bonds elongated by approximately 0.3 Å according to DFT calculations (Supporting Information, Figure S24–S26).[26] For back-intersystem crossing ($^2E \rightarrow {}^4T_2$), the large energy gap and the reorganizational barrier must be overcome which is clearly impossible at room temperature (Figure 3).[15] Direct intersystem crossing from $^4T_2$ to the vibrationally excited $^2T_1/^2E$ states or to the $^2T_2$ state and subsequent internal conversion is conceivable (Figure 3). For $Cr(acac)_3$ (acac = acetylacetonato), McCusker et al. have shown that intersystem crossing to ^2E is faster than vibrational cooling within the $^4T_2$ state along the Jahn–Teller modes.[27] Intersystem crossing might also occur from vibrationally hot states in $\mathbf{1}^{3+}$ before the Jahn–Teller distortion. Independent of the details of the intersystem crossing processes, the use of the strong-field ddpd ligand is very efficient in inducing high phosphorescence quantum yields and lifetimes as a result of the large barrier for back-intersystem crossing.[15]

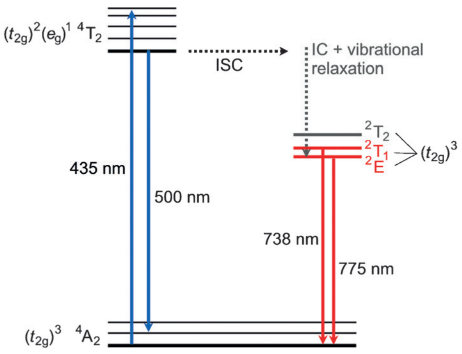

Figure 3. Jablonski diagram of $\mathbf{1}^{3+}$ constructed from experimental solution data ($^2T_2$ state tentatively from single-crystal absorption). ISC = intersystem crossing, IC = internal conversion.

As expected, the phosphorescence quantum yield is sensitive to the presence of O_2.[28,29] In air, Φ is reduced by factors of 5.2 (H_2O) and 17 (CH_3CN) and the lifetimes are correspondingly shortened from 898 µs to 177 µs (H_2O) and 51 µs (CH_3CN)(Figure 2). The bimolecular O_2 quenching constant has been estimated from a Stern–Volmer plot of **1**$(BF_4)_3$ in H_2O as $k_q = 1.77 \times 10^7\,\text{M}^{-1}\text{s}^{-1}$ and the Stern–Volmer constant as $K_{SV} = k_d \times \tau = 1.59 \times 10^4\,\text{M}^{-1}$ (Supporting Information, Figure S15). These quenching efficiencies[29] suggest possible applications of $\mathbf{1}^{3+}$ in optical oxygen sensors,[2,30] with the large difference between excitation and emission easing the combination with a spectrally distinguishable O_2-inert reference dye. The quenching efficiency is explained on the basis of the very long ^2E lifetime and on the basis of spin statistics, although k_q is not particularly large.[29c] The k_q value might be associated with an effective shielding of Cr^{III} by the ligands and the counterions (Figure 1, Figure S1). Commonly employed optical oxygen sensors are based on the quenching of their dye's excited triplet states, for example, ^3MLCT or $^3\pi\pi^*$, by $^3O_2$ yielding the dye's singlet ground state and $^1O_2$.[2,30] For these triplet states, spin statistics predict that $^1/_9$ (11%) of the possible encounters (quintet, triplet, singlet: 9 possibilities), namely the singlets, are productive. For the ^2E state of $\mathbf{1}^{3+}$ and $^3O_2$, a quartet and a doublet encounter complex is conceivable giving six microstate possibilities. The quartet encounter is productive giving the $^4A_2$ state of $\mathbf{1}^{3+}$ and $^1O_2$. Hence, $^4/_6$ (67%) of the encounters should yield $^1O_2$ which explains the O_2 sensitivity of Cr^{III} complexes in general.

The substitutional stability of $\mathbf{1}(BF_4)_3$ was probed in aqueous solution (pH 7) as well as in the presence of HCl (pH 2.1) and NaOH (pH 11.9). The cation $\mathbf{1}^{3+}$ is stable for at least 2.5 months according to UV/Vis spectroscopy (Figure S16,S17). This stability is in stark contrast to the lability of $[Cr(bpy)_3]^{3+}$ and $[Cr(tpy)_2]^{3+}$.[22] Also, $\mathbf{1}^{3+}$ is perfectly stable in 0.1 M $[nBu_4N]Cl$ and in $[nBu_4N](OH)$ (pH 11.4) H_2O/CH_3CN (1:1) solution under illumination with LEDs at 430 nm in air according to absorption and emission spectra while an isoabsorptive solution of $[Cr(bpy)_3]^{3+}$ undergoes complete photosubstitution within a few hours (Figure S18).[15] These experiments demonstrate the superior stability of $\mathbf{1}^{3+}$ compared to $[Cr(bpy)_3]^{3+}$ in aqueous solution.

Thanks to the difficult Cr^{III}/Cr^{II} reduction and the low ^2E energy, the oxidative power of the ^2E state of $\mathbf{1}^{3+}$ is rather small $[E(Cr^{III/II})^* = E(Cr^{III/II}) + E_{00}(^2E) = -1.11\,V + 1.60\,V = 0.49\,V$ versus ferrocene (+1.12 V vs. normal hydrogen electrode (NHE))]. Hence, no photooxidative damage to organic material is expected. In contrast $[Cr(bpy)_3]^{3+}$ or $[Cr(ttpy)_2]^{3+}$ photooxidize dGMP and hence, cleave DNA in their excited states (ttpy = *p*-tolylterpyridine, dGMP = deoxyguanosine monophosphate).[31] Indeed, dGMP ($E = 1.29$ V vs. NHE) quenches the emission of $[Cr(bpy)_3]^{3+}$ under our conditions but not that of $\mathbf{1}^{3+}$ (Figure S19).

Based upon rational ligand design, we could obtain the first molecular, water- or CH_3CN-soluble ruby analogues $\mathbf{1}(BF_4)_3$ and $\mathbf{1}(PF_6)_3$ with excellent phosphorescence quantum yields. Together with their high stability, their simple high-yield synthesis, their large excitation/emission energy gap and long lifetime these properties will allow a plethora of applications, such as time-gated imaging, the design of optical probes, and integration into multiplexed sensing schemes. We aim to explore their full potential in the near future.

Acknowledgements

We thank Luca Carrella and Eva Rentschler for collecting the SQUID data of $\mathbf{1}(PF_6)_3$. Parts of this research were conducted using the supercomputer Mogon and advisory services offered by Johannes Gutenberg University Mainz (www.hpc.uni-mainz.de), which is a member of the AHRP and the Gauss Alliance e.V. This work was financially supported by the Deutsche Forschungsgemeinschaft (GSC 266, Materials Science in Mainz, scholarship for C.K.).

Keywords: chromium complexes · intersystem crossing · ligand-field splitting · NIR luminescence · photophysics

How to cite: *Angew. Chem. Int. Ed.* **2015**, *54*, 11572–11576
Angew. Chem. **2015**, *127*, 11735–11739

---

[1] H. Xiang, J. Cheng, X. Ma, X. Zhou, J. Chruma, *Chem. Soc. Rev.* **2013**, *42*, 6128–6185.

[2] M. Quaranta, S. M. Borisov, I. Klimant, *Bioanal. Rev.* **2012**, *4*, 115–157.

[3] a) "Luminescent lanthanide complex, and articles and inks containing the luminescent complex": F. Thomas, C. Laporte, PCT Int. Appl. WO 2014048702A1, **2014**; b) "Secure document comprising luminescent chelates": V. Aboutanos, T. Tiller, C. Reinhard, S. Rascagnères, PCT Int. Appl. WO 2010130681A1, **2010**.

[4] A. J. Amoroso, S. J. A. Pope, *Chem. Soc. Rev.* **2015**, *44*, 4723–4742.

[5] E. Pershagen, K. E. Borbas, *Coord. Chem. Rev.* **2014**, *273–274*, 30–46.

[6] E. J. New, D. Parker, D. G. Smith, J. W. Walton, *Curr. Opin. Chem. Biol.* **2010**, *14*, 238–246.

[7] S. V. Eliseeva, J.-C. G. Bünzli, *Chem. Soc. Rev.* **2010**, *39*, 189–227.

[8] a) Q. Zhao, C. Huanga, F. Li, *Chem. Soc. Rev.* **2011**, *40*, 2508–2524; b) O. S. Wenger, *Chem. Rev.* **2013**, *113*, 3686–3733.

[9] V. W.-W. Yam, K. M.-C. Wong, *Chem. Commun.* **2011**, *47*, 11579–11592.

[10] P.-T. Chou, Y. Chi, *Chem. Eur. J.* **2007**, *13*, 380–395.

[11] Selection of examples: a) S. Wiktorowski, C. Rosazza, M. J. Winterhalder, E. Daltrozzo, A. Zumbusch, *Chem. Commun.* **2014**, *50*, 4755–4758; b) T. Marks, E. Daltrozzo, A. Zumbusch, *Chem. Eur. J.* **2014**, *20*, 6494–6504; c) D. Frath, J. Massue, G. Ulrich, R. Ziessel, *Angew. Chem. Int. Ed.* **2014**, *53*, 2290–2310; *Angew. Chem.* **2014**, *126*, 2322–2342; d) J. C. Er, C. Leong, C. L. Teoh, Q. Yuan, P. Merchant, M. Dunn, D. Sulzer, D. Sames, A. Bhinge, D. Kim, S.-M. Kim, M.-H. Yoon, L. W. Stanton, S. H. Je, S.-W. Yun, Y.-T. Chang, *Angew. Chem. Int. Ed.* **2015**, *54*, 2442–2446; *Angew. Chem.* **2015**, *127*, 2472–2476; e) S. Wiktorowski, E. Daltrozzo, A. Zumbusch, *RSC Adv.* **2015**, *5*, 29420–29423; f) D. Jänsch, C. Li, L. Chen, M. Wagner, K. Müllen, *Angew. Chem. Int. Ed.* **2015**, *54*, 2285–2289; *Angew. Chem.* **2015**, *127*, 2314–2319; g) E. Heyer, P. Lory, J. Leprince, M. Moreau, A. Romieu, M. Guardigli, A. Roda, R. Ziessel, *Angew. Chem. Int. Ed.* **2015**, *54*, 2995–2999; *Angew. Chem.* **2015**, *127*, 3038–3042; h) U. Resch-Genger, M. Grabolle, S. Cavaliere-Jaricot, R. Nitschke, T. Nann, *Nat. Methods* **2008**, *5*, 763–775.

[12] M. Schulze, A. Steffen, F. Würthner, *Angew. Chem. Int. Ed.* **2015**, *54*, 1570–1573; *Angew. Chem.* **2015**, *127*, 1590–1593.

[13] a) J. V. Caspar, E. M. Kober, B. P. Sullivan, T. J. Meyer, *J. Am. Chem. Soc.* **1982**, *104*, 630–632; b) J. V. Caspar, T. J. Meyer, *J. Am. Chem. Soc.* **1983**, *105*, 5583–5590; c) J. V. Caspar, T. J. Meyer, *J. Phys. Chem.* **1983**, *87*, 952–957; d) T. J. Meyer, *Pure Appl. Chem.* **1986**, *58*, 1193–1206.

[14] a) N. Armaroli, G. Accorsi, F. Cardinali, A. Listorti, *Top. Curr. Chem.* **2007**, *280*, 69–115; b) C. E. McCusker, F. N. Castellano, *Inorg. Chem.* **2013**, *52*, 8114–8120; c) M. S. Lazorski, F. N. Castellano, *Polyhedron* **2014**, *82*, 57–70.

[15] a) A. D. Kirk, *Chem. Rev.* **1999**, *99*, 1607–1640; b) L. S. Forster, *Coord. Chem. Rev.* **2002**, *227*, 59–92; c) N. A. P. Kane-Maguire, *Top. Curr. Chem.* **2007**, *280*, 37–67; d) V. Balzani, P. Ceroni, A.

Juris, *Photochemistry and Photophysics*, Wiley-VCH, Weinheim, **2014**, pp. 216–219; e) M. A. Jamieson, N. Serpone, M. Z. Hoffman, *Coord. Chem. Rev.* **1981**, *39*, 121–179; f) C. K. Ryu, J. F. Endicott, *Inorg. Chem.* **1988**, *27*, 2203–2214.

[16] a) T. H. Maiman, *Nature* **1960**, *187*, 493–494; b) C. Degli Esposti, L. Bizzocchi, *J. Chem. Educ.* **2007**, *84*, 1316–1318.

[17] a) A. Hauser, M. E. Von Arx, R. Pellaux, S. Decurtins, *Mol. Cryst. Liq. Cryst.* **1996**, *286*, 225–230; b) M. Milos, S. Kairouani, S. Rabaste, A. Hauser, *Coord. Chem. Rev.* **2008**, *252*, 2540–2551; c) L. Aboshyan-Sorgho, H. Nozary, A. Aebischer, J.-C. G. Bünzli, P.-Y. Morgantini, K. R. Kittilstved, A. Hauser, S. V. Eliseeva, S. Petoud, C. Piguet, *J. Am. Chem. Soc.* **2012**, *134*, 12675–12684; d) M. Cantuel, F. Gumy, J.-C. G. Bünzli, C. Piguet, *Dalton Trans.* **2006**, 2647–2660; e) S. Torelli, D. Imbert, M. Cantuel, G. Bernardinelli, S. Delahaye, A. Hauser, J.-C. G. Bünzli, C. Piguet, *Chem. Eur. J.* **2005**, *11*, 3228–3242.

[18] S. M. Stevenson, M. P. Shores, E. M. Ferreira, *Angew. Chem. Int. Ed.* **2015**, *54*, 6506–6510; *Angew. Chem.* **2015**, *127*, 6606–6610.

[19] a) H. Yersin, P. Huber, G. Gietl, D. Trümbach, *Chem. Phys. Lett.* **1992**, *199*, 1–9; b) F. Castelli, L.-S. Forster, *J. Am. Chem. Soc.* **1975**, *97*, 6306–6309.

[20] a) N. Sabbatini, V. Balzani, *J. Am. Chem. Soc.* **1972**, *94*, 7587–7589; b) H. F. Wasgestian, *J. Phys. Chem.* **1972**, *76*, 1947–1951.

[21] a) A. Breivogel, C. Förster, K. Heinze, *Inorg. Chem.* **2010**, *49*, 7052–7056; b) K. Mack, A. Wünsche von Leupoldt, C. Förster, M. Ezhevskaya, D. Hinderberger, K. W. Klinkhammer, K. Heinze, *Inorg. Chem.* **2012**, *51*, 7851–7858; c) A. Breivogel, M. Meister, C. Förster, F. Laquai, K. Heinze, *Chem. Eur. J.* **2013**, *19*, 13745–13760; d) C. Förster, K. Mack, L. M. Carrella, V. Ksenofontov, E. Rentschler, K. Heinze, *Polyhedron* **2013**, *52*, 576–581; e) A. Breivogel, M. Park, D. Lee, S. Klassen, A. Kühnle, C. Lee, K. Char, K. Heinze, *Eur. J. Inorg. Chem.* **2014**, 288–295; f) A. Breivogel, C. Kreitner, K. Heinze, *Eur. J. Inorg. Chem.* **2014**, 5468–5490; g) A. K. C. Mengel, C. Förster, A. Breivogel, K. Mack, J. R. Ochsmann, F. Laquai, V. Ksenofontov, K. Heinze, *Chem. Eur. J.* **2015**, *21*, 704–714.

[22] a) M. Maestri, F. Bolletta, N. Serpone, L. Moggi, V. Balzani, *Inorg. Chem.* **1976**, *15*, 2048–2051; b) E. C. Constable, C. E. Housecroft, M. Neuburger, J. Schönle, J. A. Zampese, *Dalton Trans.* **2014**, *43*, 7227–7235.

[23] a) C. C. Scarborough, K. M. Lancaster, S. DeBeer, T. Weyhermüller, S. Sproules, K. Wieghardt, *Inorg. Chem.* **2012**, *51*, 3718–3732; b) C. C. Scarborough, S. Sproules, T. Weyhermüller, S. Serena DeBeer, K. Wieghardt, *Inorg. Chem.* **2011**, *50*, 12446–12462.

[24] U. Casellato, R. Graziani, R. P. Bonomo, A. J. Di Bilio, *J. Chem. Soc. Dalton Trans.* **1991**, 23–31.

[25] N. A. P. Kane-Maguire, J. Conway, C. H. Langford, *J. Chem. Soc. Chem. Commun.* **1974**, 801–802.

[26] a) F. Gilardoni, J. Weber, K. Bellafrouh, C. Daul, H. U. Güdel, *J. Chem. Phys.* **1996**, *104*, 7624–7632; b) O. S. Wenger, H. U. Güdel, *J. Chem. Phys.* **2001**, *114*, 5832–5841.

[27] a) E. A. Juban, J. K. McCusker, *J. Am. Chem. Soc.* **2005**, *127*, 6857–6865; b) E. A. Juban, A. L. Smeigh, J. E. Monat, J. K. McCusker, *Coord. Chem. Rev.* **2006**, *250*, 1783–1791.

[28] a) N. Serpone, M. A. Jamieson, M. S. Henry, M. Z. Hoffman, F. Bolletta, M. Maestri, *J. Am. Chem. Soc.* **1979**, *101*, 2907–2916; b) B. Brunschwig, N. Sutin, *J. Am. Chem. Soc.* **1978**, *100*, 7568–7577.

[29] a) M. Isaacs, A. G. Sykes, S. Ronco, *Inorg. Chim. Acta* **2006**, *359*, 3847–3854; b) K. D. Barker, K. A. Barnett, S. M. Connell, J. W. Glaeser, A. J. Wallace, J. Wildsmith, B. J. Herbert, J. F. Wheeler, N. A. P. Kane-Maguire, *Inorg. Chim. Acta* **2001**, *316*, 41–49; c) M. Z. Hoffman, F. Bolletta, L. Moggi, G. L. Hug, *J. Phys. Chem. Ref. Data* **1989**, *18*, 219–543.

[30] J. Napp, T. Behnke, L. Fischer, C. Würth, M. Wottawa, D. M. Katschinski, F. Alves, U. Resch-Genger, M. Schäferling, *Anal. Chem.* **2011**, *83*, 9039–9046.

[31] a) R. T. Watson, N. Desai, J. Wildsmith, J. F. Wheeler, N. A. P. Kane-Maguire, *Inorg. Chem.* **1999**, *38*, 2683–2687; b) V. G. Vaidyanathan, B. U. Nair, *Eur. J. Inorg. Chem.* **2004**, 1840–1846.

Received: May 29, 2015